Research Article
Viral Hepatitis

JOURNAL
OF HEPATOLOGY

Multi-parametric analysis of human livers reveals variation in intrahepatic inflammation across phases of chronic hepatitis B infection

Graphical abstract

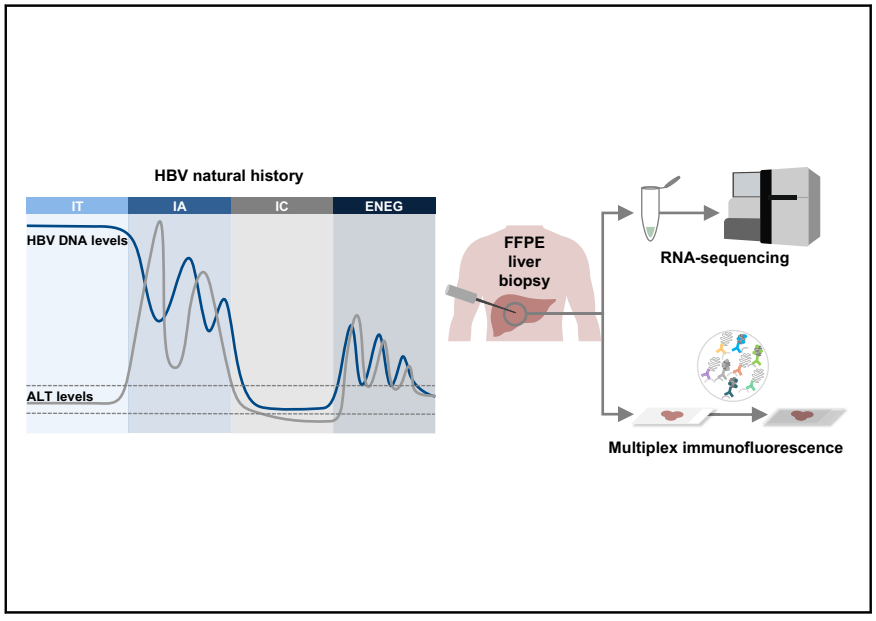

Highlights

- RNA-Seq and multiplex immunofluorescence (mIF) was performed on liver biopsies to characterize the HBV clinical phases.
- Chronic HBV livers were characterized by higher immune-gene expression and leukocyte infiltrate than healthy livers.
- ALT determined immune gene expression profiles in livers of IA and ENEG patients.
- Immune-exhaustion profiles were observed in livers of IA and ENEG patients.
- Leukocyte infiltrate correlated with serum ALT, but not with HBV DNA or intrahepatic HBcAg and HBsAg.

Authors

Noe Rico Montanari, Ricardo Ramírez, Abhishek Aggarwal, …, Jose D. Debes, Becket Feierbach, Andre Boonstra

Correspondence

p.a.boonstra@erasmusmc.nl (A. Boonstra).

Lay summary

Immunological studies on chronic HBV remain largely restricted to assessment of peripheral responses due to the limited access to the site of infection, the liver. In this study, we comprehensively analyzed livers from a well-defined cohort of patients with chronic HBV and uninfected controls with state-of-the-art techniques, and evaluated the differences in gene expression profiles and inflammation characteristics across distinct disease phases in patients with chronic HBV.

https://doi.org/10.1016/j.jhep.2022.02.016
 J. Hepatol. 2022, 77, 332–343

Research Article
Viral Hepatitis

JOURNAL OF HEPATOLOGY

Multi-parametric analysis of human livers reveals variation in intrahepatic inflammation across phases of chronic hepatitis B infection

Noe Rico Montanari[1,†], Ricardo Ramírez[2,†], Abhishek Aggarwal[2,†], Nick van Buuren[2], Michael Doukas[3], Christina Moon[2], Scott Turner[2], Lauri Diehl[2], Li Li[2], Jose D. Debes[1,4], Becket Feierbach[2,#], Andre Boonstra[1,*,#]

[1]*Department of Gastroenterology and Hepatology, Erasmus University Medical Center, Rotterdam, The Netherlands;* [2]*Gilead Sciences, Foster City, CA, USA;* [3]*Department of Pathology, Erasmus University Medical Center, Rotterdam, The Netherlands;* [4]*Department of Medicine, Division of Gastroenterology & Division of Infectious Diseases, University of Minnesota, Minneapolis, MN, USA*

Background & Aims: Chronic HBV is clinically categorized into 4 phases by a combination of serum HBV DNA levels, HBeAg status and alanine aminotransferase (ALT): immunotolerant (IT), immune-active (IA), inactive carrier (IC) and HBeAg-negative hepatitis (ENEG). Immune and virological measurements in the blood have proven useful but are insufficient to explain the interrelation between the immune system and the virus since immune dynamics differ in the blood and liver. Furthermore, the inflammatory response in the liver and parenchymal cells cannot be fully captured in blood.

Methods: Immunological composition and transcriptional profiles of core needle liver-biopsies in chronic HBV phases were compared to those of healthy controls by multiplex immunofluorescence and RNA-sequencing (n = 37 and 78, respectively) analyses.

Results: Irrespective of the phase-specific serological profiles, increased immune-gene expression and frequency was observed in chronic HBV compared to healthy livers. Greater transcriptomic deregulation was seen in IA and ENEG (172 *vs.* 243 DEGs) than in IT and IC (13 *vs.* 35 DEGs) livers. Interferon-stimulated genes, immune-activation and exhaustion genes (*ICOS*, *CTLA4*, *PDCD1*) together with chemokine genes (*CXCL10*, *CXCL9)* were significantly induced in IA and ENEG livers. Moreover, distinct immune profiles associated with ALT elevation and a more accentuated immune-exhaustion profile (*CTLA4*, *TOX*, *SLAMF6*, *FOXP3*) were observed in ENEG, which set it apart from the IA phase *(LGALS9*, *PDCD1*). Interestingly, all HBV phases showed downregulation of metabolic pathways *vs.* healthy livers (fatty and bile acid metabolism). Finally, increased leukocyte infiltrate correlated with serum ALT, but not with HBV DNA or viral proteins.

Conclusion: Our comprehensive multi-parametric analysis of human livers revealed distinct inflammatory profiles and pronounced differences in intrahepatic gene profiles across all chronic HBV phases in comparison to healthy liver.

Lay summary: Immunological studies on chronic HBV remain largely restricted to assessment of peripheral responses due to the limited access to the site of infection, the liver. In this study, we comprehensively analyzed livers from a well-defined cohort of patients with chronic HBV and uninfected controls with state-of-the-art techniques, and evaluated the differences in gene expression profiles and inflammation characteristics across distinct disease phases in patients with chronic HBV.

Introduction

Chronic hepatitis B is a heterogeneous disease which progresses through distinct disease phases that differ in the levels of viral replication and the degree of liver damage inflicted by immune responses against hepatocytes infected with HBV.[1] Four phases have been defined on the basis of the variable serum levels of HBV DNA, HBeAg and alanine aminotransferase (ALT): immunotolerant (IT), immune-active (IA), inactive carrier (IC) and HBeAg-negative hepatitis (ENEG).[2] The distinction between phases is clinically relevant as it determines the indication for antiviral treatment, aimed at reducing viral replication and liver damage in the IA and ENEG phases.[3]

HBV is a non-cytopathic virus, meaning that the liver damage observed during the chronic phase of the disease is a direct consequence of the immune response against the virus.[3] Histopathological evaluation of the liver of infected patients demonstrated that mild leukocyte infiltration is observed in the IT and IC phases, whereas extensive infiltrates are observed in the IA and ENEG phases, predominantly in the portal tract area.[4] These distinct characteristics were used by European Association for the Study of the Liver (EASL) to propose a revised nomenclature for HBeAg-positive and HBeAg-negative chronic HBV: chronic infection *vs.* chronic hepatitis, which is thought to better describe the phases.[3]

In recent years, several studies have examined the immunological and virological differences between the natural phases of

Keywords: HBV; liver biopsy; RNA-Seq; liver; inflammation; tissue; immunology.
Received 19 October 2021; received in revised form 31 January 2022; accepted 13 February 2022; available online 24 February 2022

* Corresponding author. Address: Erasmus MC, University Medical Center Rotterdam, 3015 CE, Rotterdam, the Netherlands.
E-mail address: p.a.boonstra@erasmusmc.nl (A. Boonstra).
† Equal contribution.
# Equal contribution.

https://doi.org/10.1016/j.jhep.2022.02.016

chronic HBV infection. Most of these studies have examined the peripheral compartment where minor differences were reported in the frequencies and phenotype of circulating natural killer (NK) cells, T cells and B-cells when comparing blood samples from patients at different clinical phases.[5–7] However, since HBV replication takes place in the liver, assessment of the intrahepatic immune response will provide a more accurate evaluation of the local antiviral and inflammatory processes in the HBV-infected liver.[8] Moreover, it is well described that the number, phenotype and function of immune cells, differs between the liver and blood.[9–11] To date, no studies have systematically evaluated differences in chronic HBV livers at the distinct clinical phases by means of immunological techniques, such as flow cytometry, and only few studies have reported differences at the gene expression level of livers at distinct clinical phases using core needle biopsies collected for diagnostic purposes. Two studies compared the intrahepatic gene expression by microarray in patients with chronic HBV, with respect to the first phase in chronic disease (IT phase) as a control and showed increased immune gene expression during chronic hepatitis phases, albeit relatively modest in number compared to chronic infection phases.[12,13] A third study by Lebossé *et al.* using Taqman low densities array technology, highlighted a general downregulation of innate immune genes in patients with chronic HBV compared to non-HBV-infected patients.[14] However, these studies did not include true uninfected healthy controls, and lack information on immune cell infiltrates in the infected livers.

To better understand the intrahepatic processes underlying viral replication and immune control, it will be critical to characterize the intrahepatic immune milieu in HBV-infected livers across different phases. To provide a global molecular profile of each phase, we combined state-of-the-art RNA-sequencing (RNA-seq) and whole tissue multiplex immunofluorescence microscopy on core needle liver biopsies from a unique cohort of uninfected healthy controls and patients with chronic HBV across the different clinical phases of the disease. This approach allowed us to assess the intrahepatic host-virus interplay by elucidating the level and make up of leukocyte infiltrates and host gene expression in relation to the degree of inflammation and HBV antigen burden in the liver. Contrary to previous observations, we observed a prevalent downregulation of metabolic genes and pathways across all chronic HBV phases and a general upregulation of innate and adaptive immune genes and pathways in chronic HBV, particularly in chronic-hepatitis phases. Moreover, we detected increased gene expression of immune-exhaustion genes in chronic hepatitis phases. Lastly, leukocyte infiltration was predominantly restricted to portal and peri-portal areas and only associated with the inflammation level (ALT) but not with the positivity for intrahepatic HBV antigens (HBcAg and HBsAg) or replication activity (serum HBV DNA).

Material and methods

Patients and liver samples

Formalin fixed paraffin embedded (FFPE) core needle liver biopsies from 69 patients with chronic HBV and 9 healthy controls were used for RNA-seq (Table 1), and biopsies from a matched subset of patients with chronic HBV (n = 30) and healthy controls (n = 7) were used for multiplex immunohistochemistry (Table S1). The livers of healthy individuals were collected to determine their eligibility as altruistic liver donors. All other liver biopsies were collected as part of routine clinical care at the Erasmus MC and archived. Patients were classified as IT, IA, IC or ENEG based on their serum HBV DNA, ALT levels and HBeAg status. An ALT of 30 IU/ml was considered normal and chronic hepatitis phases, IA and ENEG, were determined using a threshold of 1.5x the upper limit of normal for ALT and/or 20,000 IU/ml for HBV DNA, alongside the HBeAg status (positive and negative, respectively). Patients received neither antiviral treatment prior to biopsy, nor had any co-existing primary liver disease, nor were co-infected with HCV, HEV, HDV or HIV. Histological evaluation of METAVIR staging was performed as described previously by a single liver pathologist in a uniform manner.[15] Due to the retrospective nature of this study, written informed consent was not obtained from each patient. Instead, the ethical review board of the Erasmus MC approved this study as it was in accordance with the COREON guidelines, which describes the use of coded-anonymous residual human tissue for scientific research (www.coreon.org).

FFPE liver RNA extraction and transcriptome sequencing

Eight 10 μm-thick core needle liver biopsies were sectioned, deparaffinized, and total RNA was isolated using the RNeasy FFPE Kit (Qiagen, Germany) following the manufacturer's instructions. Prior to library preparation, rRNA was depleted using the Illumina Ribo-Zero rRNA Depletion kit (Illumina, USA) following the

Table 1. Patient characteristics of liver biopsies included in the RNA-sequencing analysis.

	Healthy control	IT (chronic infection HBeAg+)	IA (chronic hepatitis HBeAg+)	IC (chronic infection HBeAg-)	ENEG (chronic hepatitis HBeAg-)
N samples	9	15	15	23	16
Age (Median, IQR)	52 (28-57)	24 (18-32)	24 (18-27)	35 (29-45)	35 (24-45)
Male, n (%)	4 (44%)	4 (26%)	5 (33%)	10 (43%)	13 (81%)
ALT (IU/ml) (Median, IQR)	24 (22-45)	29 (21–50)	68 (46-164)	27 (21–32)	101 (61–222)
Log_{10} HBV DNA (IU/ml) (Median, IQR)	n.a.	8.6 (8.1–8.8)	8.6 (7.4–8.7)	2.2 (<1–2.9)	6.0 (4.0–8.3)
HBeAg-positive, n (%)	n.a.	15 (100%)	15 (100%)	0 (0%)	0 (0%)
Anti-HBeAg antibody positive, n (%)	n.a.	0 (0%)	0 (0%)	23 (100%)	16 (100%)
HBV genotype, n (%)	n.a.				
A		1 (7%)	1 (6%)	4 (17%)	2 (12%)
B		4 (27%)	3 (18%)	3 (13%)	2 (12%)
C		8 (53%)	7 (46%)	2 (9%)	2 (12%)
D		2 (13%)	3 (18%)	10 (43%)	7 (44%)
E		0 (0%)	1 (6%)	1 (4%)	2 (12%)
ND		0 (0%)	0 (0%)	3 (13%)	1 (6%)
Fibrosis ≤F2, n (%) (METAVIR)	9 (100%)	14 (93%)	15 (100%)	23 (100%)	13 (81%)

ALT, alanine aminotransferase; ENEG; HBeAg-negative hepatitis; IA, immune-active; IC, inactive carrier IT, immunotolerant.; ND, not determined.

manufacturer's instructions, and fragmented into approximately 300 base pairs. cDNA libraries for each sample were prepared using Illumina TrueSeq Total Gold. Libraries were sequenced at EA Genomics (Q^2 solutions, USA) using 100 bp paired-end reads on Illumina HiSeq platform aimed at 50 million reads per sample. Samples with less than 10 million protein-coding reads were excluded from the analysis. Sequencing fastq files will be publicly available at https://www.ncbi.nlm.nih.gov/geo/ and upon reasonable request.

Ribo-depletion RNA-seq on liver biopsies from healthy individuals and patients with chronic HBV

Raw paired-end reads were aligned to human reference genome hg38 downloaded from the USCS Genome Bioinformatics site using the STAR (v.2.7.3a).[16] Picard tools were employed to detect at least 10 million reads in protein coding mRNA regions for downstream analysis.[17] Quantification of gene expression was calculated using featureCounts (v.1.4.6-p1), converted to reads per kilobase per million mapped reads (RPKM) using the R package edgeR.[18] Subsequently, scores were calculated for gene sets from MSigDB v7 using the R GSVA package.[19,20] Gene counts per sample were used to perform differential gene expression analysis between groups using the DESeq2 package (v.1.30.1).[21] Weakly expressed genes across samples were removed from downstream analysis when 50 or less counts were detected in 4 samples per experimental group. Genes were considered as differentially expressed if adjusted p values were <0.05 and fold change was |>1.5|. Remaining genes were normalized using the estimateSizeFactors function. Hallmark and gene ontology biological process (BP) pathway analysis were conducted with gene set-enrichment analysis (GSEA) java software (v.4.1.0)[22] using the default settings "signal2noise" for ranking genes. To estimate immune cell proportions, we supplied RPKM values to the EPIC algorithm in the immunedeconv R package (v2.0.4).[23,24] Single sample gene set scores for visualization were calculated using GSVA.[20] Reads were also aligned to a combined HBV and hg38 reference sequencing using Burrows-Wheeler Aligner. Reads with at least 25 base pair alignment to the HBV genome were included to calculate HBV burden. Reads with segments mapping to both HBV and hg38 were considered chimeric reads suggesting HBV integration.

Multiplex immunofluorescence assay and image analysis

To investigate the liver immune microenvironment and viral antigen expression, FFPE liver biopsy sections, collected from patients at distinct HBV clinical phases (Table S1), were subjected to a novel multiplex immunofluorescence (mIF) technology, InSituPlex (Ultivue Inc., USA).[25–27] The custom panel used 3 iterative imaging cycles to detect 12 analytes using a cocktail of primary antibodies conjugated to unique DNA-barcodes (Fig. S1). These antibody conjugates were used to identify the protein targets using fluorescently labeled probes, complementary to the barcodes. Between imaging rounds, a gentle dehybridization step was used to remove fluorescent probes from the previous round followed by incubation of the next set of fluorescent probes. Stained slides were scanned at 20X on the AxioScan SpectraX whole slide scanner (Zeiss, Germany) followed by an H&E stain. Images were co-registered with the UltiStacker software (Ultivue, USA) using DAPI as references from the different rounds. H&E images were digitally annotated guided by a board-certified pathologist, to define the liver tissue region. H&E and mIF channels were assessed at individual marker level for suitability of analysis including staining specificity, tissue integrity and presence of artefacts. Whole slide digital image analysis was performed using Visiopharm software (v.21.2.0.9368, OracleBio, UK) to generate cell phenotype data. Single cells were identified using DAPI for nuclear detection and NaKATPase was additionally used for hepatocyte formation. Customized cellular analysis algorithms were developed to detect and phenotype individual cells by setting the threshold to ensure only a true signal was being detected by the algorithm.

Statistical analysis

Statistical analyses of clinical and virological parameters were performed with GraphPad Prism (v9) software. Baseline variables between cohorts were compared with the use of chi-square tests for categorical variables, Mann-Whitney test or (unpaired) t test for continuous variables, unless otherwise indicated. All reported p values are 2-sided. Significant differences were considered in all cases when p <0.05. Spearman/Pearson correlations were considered significant when p <0.05.

Results

Immune genes and inflammatory pathways are enriched in HBV livers with chronic inflammation (IA and ENEG), whereas metabolic pathways are suppressed

Detailed knowledge of the immune and antiviral responses that act during the distinct HBV clinical phases in chronically infected patients is essential to better understand the processes that underlie the fluctuations in viral replication and liver damage.

To study this, we performed RNA-seq on liver biopsies from 69 patients with chronic HBV at the different phases (15 IT, 15 IA, 23 IC and 16 ENEG) and compared them to biopsies obtained from 9 individuals who volunteered as altruistic liver donors (Table 1). In agreement with EASL guidelines, phase-specific serological profiles were observed across chronic HBV based on HBV DNA, ALT and HBeAg. Serum HBV DNA levels in HBeAg-positive phases (IT and IA) were the highest (mean HBV DNA >8Log10) with limited inter-patient heterogeneity within each phase (SD <1Log10). In contrast, the ENEG phase was characterized by lower HBV DNA levels than HBeAg-positive phases (mean HBV DNA 6 Log10) but with greater heterogeneity (SD >2Log10). In contrast, serum HBV load in almost half of the IC patients (10/23) was undetectable, and in all but one patient displaying HBV DNA levels (<4Log10) (Fig. S2). Moreover, serum ALT levels were within the normal range in patients classified in the IT and IC phase (mean <35 IU/ml) whereas patients classified in the IA and ENEG phases displayed elevated serum ALT levels (mean 126 and 208 IU/ml, respectively, clearly showing signs of ongoing liver inflammation (Fig. S2).

Comparison of the liver transcriptome across the distinct HBV clinical phases to healthy livers highlighted a large disparity in the number of differentially expressed genes (DEGs; adjusted p <0.05 and fold change |>1.5|). Although the patients in the IT and IC phase exhibit high variability in HBV DNA and HBeAg, their intrahepatic gene expression profile was comparable with a relatively low number of DEGs, 13 and 35 DEGs, respectively (Fig. 1A and S3, Table S2). In contrast, livers from IA and ENEG patients displayed 172 and 243 DEGs, respectively, with almost 70% of them being upregulated in chronic HBV compared to healthy livers (Fig. 1A and S3, Table S2). Interestingly, this profile was comparable in all IA and ENEG patients (Fig. 1B), despite the fact that serum ALT levels were highly variable (Fig. S2). As shown

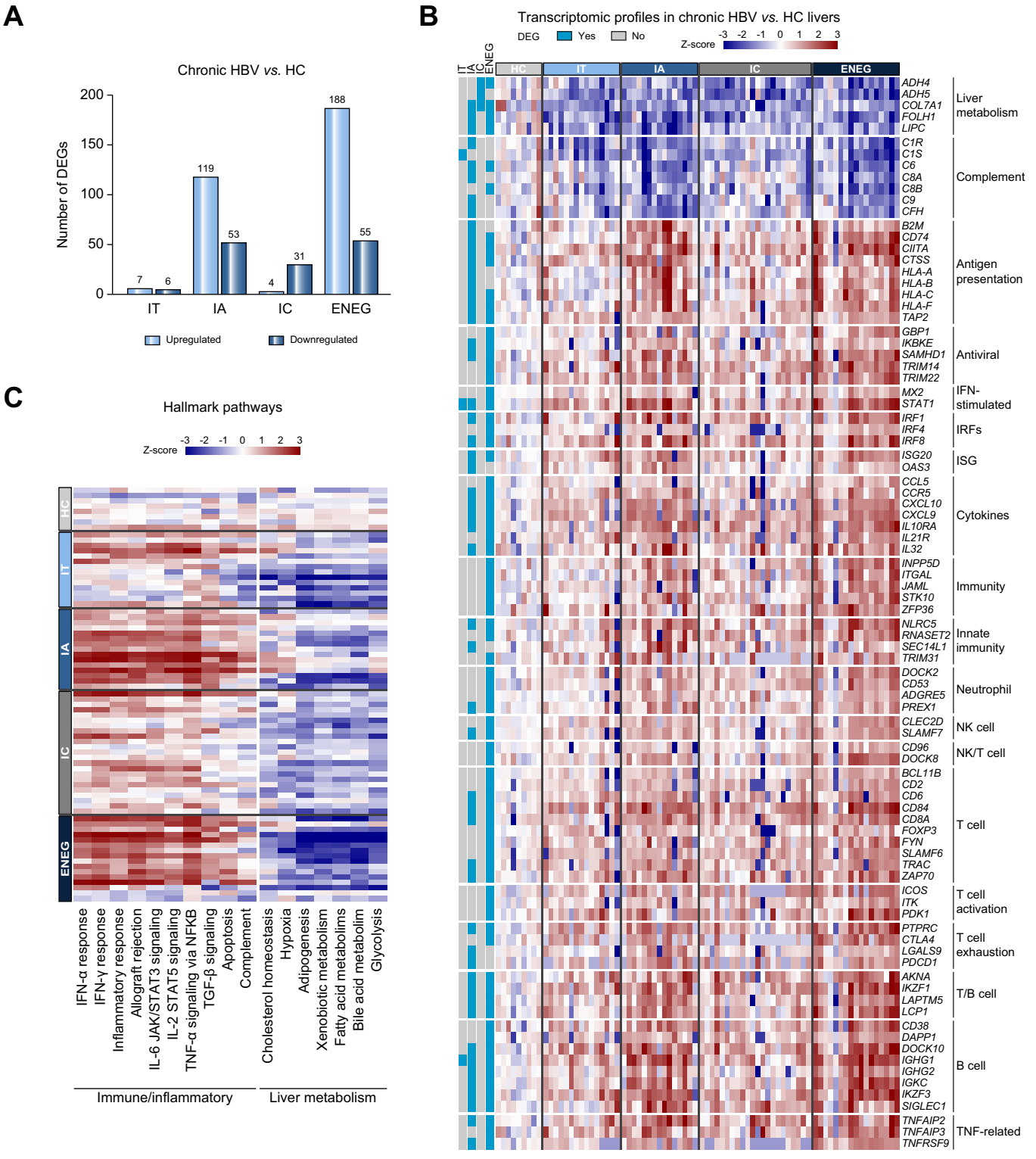

Fig. 1. Increased immune gene expression and inflammatory pathways in chronic HBV livers. (A) Bar plot representing the number of DEGs (adjusted p <0.05 AND fold change |>1.5|) in each chronic HBV phase compared to the HC group. Red and blue bars represent upregulated and downregulated genes, respectively. (B) Heatmap depicting z-scores from metabolic, innate and adaptive immune genes in HC and patients with chronic HBV. Scaling was conducted per gene (row) using the mean gene expression in the HC group. DEGs in chronic HBV (IT, IA, IC and ENEG) phases compared to HC are indicated highlighted in blue (left side). (C) Heatmap depicting z-scores of selected Hallmark pathways categorized as Immune/inflammatory and liver-metabolism across HC and chronic HBV livers. Scaling was conducted per pathway (column) using the mean pathway score in the HC. Positive and negative z-scores in panel B and C heatmaps are colored in gradients of red and blue, respectively. DEGs, differentially expressed genes; ENEG; HBeAg-negative hepatitis; HC, healthy control; IA, immune-active; IC, inactive carrier IT, immunotolerant.

in Fig. 1B, livers from all 4 phases of chronic HBV demonstrated a common downregulation of genes involved in metabolic processes (*ADH4*, *ADH5*, *LIPC* and *FOLH1*) and complement system (classical pathway [*C1R* and *C1S*] and MAC attack complex [*C6*, *C8A* and *C8B*]). Of note, all phases in chronic HBV, except IT, displayed decreased expression of albumin (*ALB*) (Table S2).

Besides a downregulation of metabolic genes, we also observed increased immune gene expression in livers from patients with chronic HBV compared to healthy livers; this effect was most pronounced in IA and ENEG phases (Fig. 1B). In the IT phase only *STAT1* and immunoglobulin-related gene *IGHG1* were found to be significantly increased, whereas only *GBP5* was found to be induced in IC livers when compared to healthy livers (Fig. 1B Table S2). In contrast, among the upregulated DEGs found in the IA and ENEG phases, we identified multiple overlapping genes linked to both the innate and adaptive arms of the immune system (Fig. 1B). Several HLA genes (*HLA-A/B/C*), antigen presentation genes (*CD74*, *CIITA* and *TAP*), interferon-stimulated genes (ISGs; *STAT1*, *ISG20*), interferon-regulatory factors (IRFs; *IRF1* and *IRF8*) and genes with known antiviral function such as *IKBKE* and *SAMHD1* were detected. Furthermore, we observed an upregulation of cytokine-related genes involved in inflammatory processes, such as *CXCL9* and *CXCL10* together with *IL-32* and interleukin receptor *IL10RA*. Multiple genes related to different leukocyte populations, such as neutrophils (*CD53* and *PREX1*), NK cells (*CLDC2D* and *CD96*), T cells (*ZAP70*, *CD8*, *CD2*) and B cells (*IGHG1*, *IGHG2*, *SIGLEC1*) showed increased gene expression in inflammation phases, with the strongest signal in the ENEG group, in comparison to healthy livers (Fig. 1B). Most striking was the detection of genes encoding molecules pivotal for T-cell activation upon T-cell receptor engagement, such as *ICOS*, *PDK1*, *ITK* and *THEMIS*. Furthermore, we also observed a strong upregulation of genes encoding for immune exhaustion markers expressed on exhausted T cells, such as *CTLA4*, *LGALS9*, *PDCD1* encoding for PD-1, *TNFRS19* encoding for 4-IBB, *SLAM-6* and NK-cell associated *SLAMF7* among others. Also increased expression of the genes encoding the transcription factors *TOX*, expressed in exhausted T cells, and *FOXP3*, expressed in regulatory T cells, was observed.

Next, we assessed whether the findings at the individual gene level were supported by Hallmark GSEA. Indeed, GSEA identified a general upregulation of inflammatory (inflammatory response, IL-6 JAK/STAT3 signaling) and IFN-associated (IFN-α/γ) gene sets in chronic HBV compared to healthy livers, although it was only significant in IA and ENEG phases (false discovery rate [FDR] <0.05; Fig. 1C). Moreover, in line with the findings at the individual gene level, metabolic gene sets related to adipogenesis, fatty and bile acid and xenobiotic metabolism were all significantly downregulated in all phases of chronic HBV compared to healthy livers (Fig. 1C). In with chronic HBV display a downregulation of numerous metabolic genes in all 4 clinical HBV phases. Moreover, livers from the IA and ENEG phase exhibit a relatively strong increase in differentially expressed immune genes and inflammatory pathways compared to healthy livers, while this increase is minimal in IT and IC livers.

Livers from IA and ENEG phases display considerable transcriptional overlap yet distinct patterns correlate with ALT

To further characterize intrahepatic transcriptomic profiles in the different phases of chronic HBV, we performed GSEA on BP from gene ontology pathways, which contains an extensive list of additional immune and non-immune gene sets. In line with the Hallmark GSEA, a core group of metabolic BPs (organic acid catabolism, detoxification, fatty acid metabolism and cellular respiration) was found to be significantly downregulated (FDR <0.05) in all chronic HBV phases, except the IA phase (FDR ≈0.06), when compared to healthy livers (Fig. 2A). In contrast, no BPs were upregulated in the IT and IC group compared to the healthy livers. As depicted in Fig. 2A and 2B, several of the downregulated BPs were found to overlap between the IT and IC phase (Fig. 2A-B, Table S3 and S4 for IT and IC *vs.* HC, respectively. Overlapping BPs are highlighted in yellow).

In contrast to the IT and IC livers, BPs identified in livers from IA and ENEG patients were almost all upregulated and exhibited a significant increase in those related to leukocyte activation (NK cell, T cell, B cell), neutrophil chemotaxis and immune-activation terms compared to the healthy group (Fig. 2A, Table S5 and S6 for IA and ENEG *vs.* HC, respectively). Likewise, a high number of BP terms overlapped (n = 202, 63%) between the IA and ENEG phase (Table S5 and S6 highlighted in yellow).

Although the direct GSEA comparison between IA and ENEG samples yielded no differences in BPs (not shown), the observed subtle differences in enriched BPs in IA and ENEG compared to the healthy group made us consider whether both phases could be distinguished by their individual gene expression profile on the basis of the upregulated DEGs. In line with the general overlap seen in immune activation Hallmark gene sets and BP terms, we found almost 40% overlap (n = 83) of DEGs between phases (Fig. 2C, Table S7). A good representation of these common genes was found in those encoding for the inflammatory chemokines IP-10 (*CXCL10*) and MIG (*CXCL9*) together with immune-activation (*RELT*, *STAT1* and *IRF1*) and T cell-related genes (*CD8A, CD84*), all indicative of the ongoing inflammation during these active phases. On the other hand, 36 (16%) and 105 (47%) of the DEGs were exclusively increased in IA and ENEG when compared to the healthy group, respectively. Interestingly, livers of patients in the ENEG phase displayed a higher abundance of genes participating in T-cell activation (*ICOS*, *BTN3A1*, *BTN3A2*) or T-cell immune-exhaustion (*CTLA4*, *TOX*, *FOXP3*, *CD38* and *SLAMF6*) than those found in livers from IA patients (*PDCD1* and *LGALS9*) (Fig. 2C, Table S7).

Having observed the minor but significant differences in transcriptomics in IA and ENEG livers with respect to healthy livers, we assessed whether specific gene expression profiles of IA and ENEG livers were associated with serum ALT levels. Indeed, we identified 30 and 32 candidate genes in the IA and ENEG group, respectively, associated with ALT (Rho >0.5), where only *CXCL9*, *GBP5* and *APOL3* correlated in both phases (Fig. 2D). Interestingly, ALT correlations with genes related to T cell-related activation and exhaustion were more often found in livers from ENEG patients (*BTN3A1*, *ITK*, *TRAC*, *TOX*, *SLAMF7*, *SLAMF6*) than IA patients (*ZAP70* and *LGALS9*). Taken together, these results highlight 2 major distinct profiles in chronic HBV based on the inflammation status, yet subtle and significant differences discriminate IA and ENEG chronic hepatitis phases with an even greater immune exhausted gene expression phenotype in ENEG.

Leukocyte infiltration is increased across chronic HBV natural history and correlates with serum ALT levels but not HBV DNA

Gene expression analysis at the individual gene level and GSEA analysis on BP pathways showed increased expression of leukocyte-related genes and leukocyte activation gene sets in chronic HBV phases, particularly the IA and ENEG phases, which

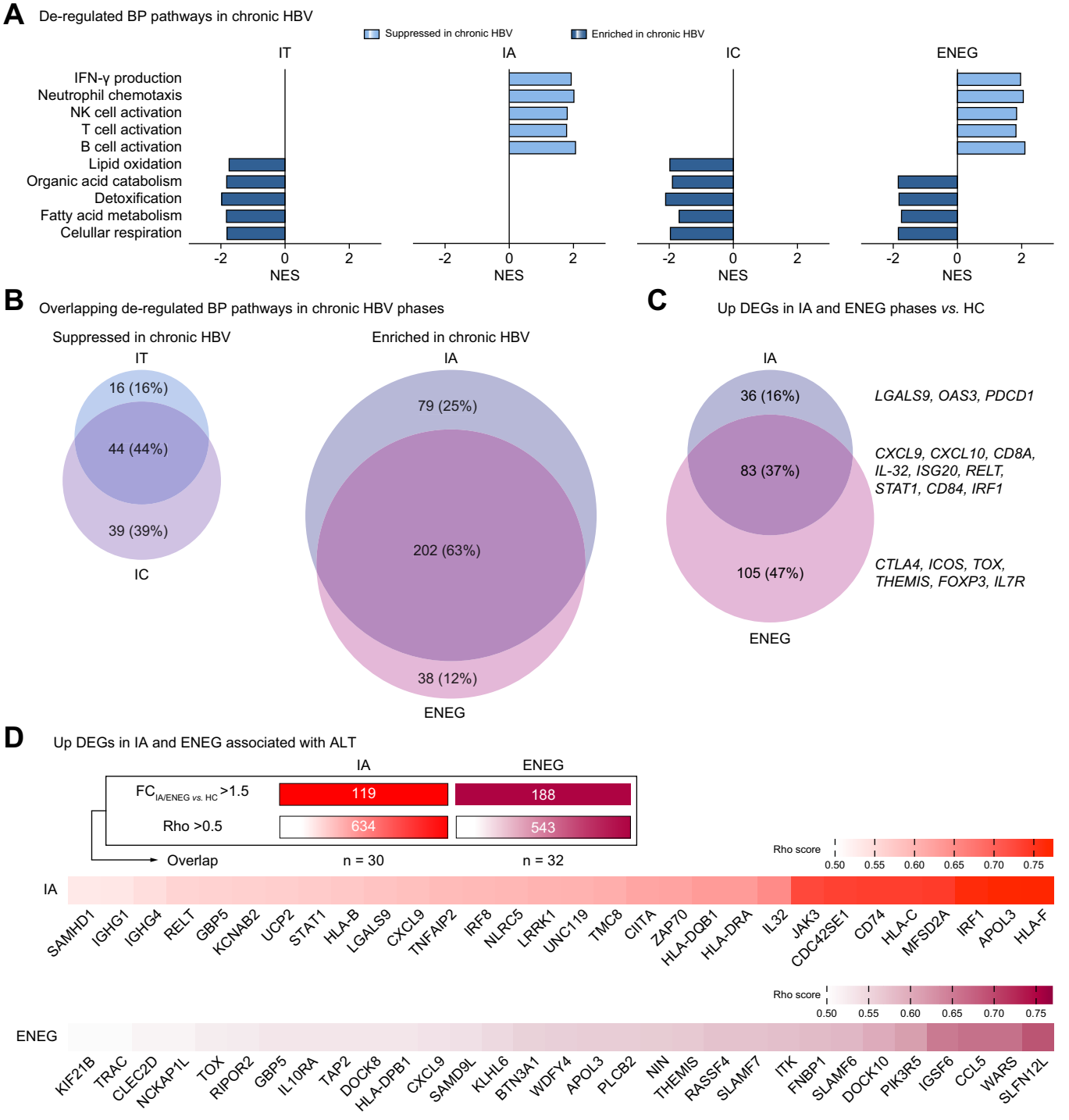

Fig. 2. Distinct intrahepatic transcriptomic profiles associated with ALT elevation, and more accentuated immune exhaustion gene profile found in ENEG compared to the IA livers. (A) Bar plots displaying NES of 10 significantly de-regulated (adjusted p <0.05) gene ontology BP pathways in chronic HBV phases compared to HC. Red and blue bars represent pathways enriched and suppressed in chronic HBV phases, respectively. (B) Venn-diagrams with number and percentage of (non-) overlapping BP pathways downregulated in IT and IC or induced in IA and ENEG when compared to HC. (C) Venn-diagram indicating the number of (non-)overlapping DEGs (fold change >1.5 and adjusted p <0.05) upregulated in IA and/or ENEG compared to HC. (D) Overlap of DEGs upregulated in livers at the IA or ENEG phase *vs.* HC livers, and significant and positively associated (p <0.05 and Spearman Rho >0.5) with ALT values within IA or ENEG. Color-gradient bars indicate increased Rho scores. ALT, alanine aminotransferase; BP, biological process; DEGs, differentially expressed genes; ENEG; HBeAg-negative hepatitis; HC, healthy control; IA, immune-active; IC, inactive carrier IT, immunotolerant; NES, normalized enrichment scores.

are well known to exhibit more pronounced liver inflammation than the IT and IC phases. To further determine if these findings translated at the protein level, we executed a mIF assay by which to detect multiple analytes on a single FFPE slide, enabling us to phenotype the lymphocyte subsets. We stained a cohort of 37 liver biopsies, a subset of the original cohort, across the natural history in chronic HBV – characterized by <F1 and ≤5% steatosis – and compared them to the healthy liver tissues (at least 7

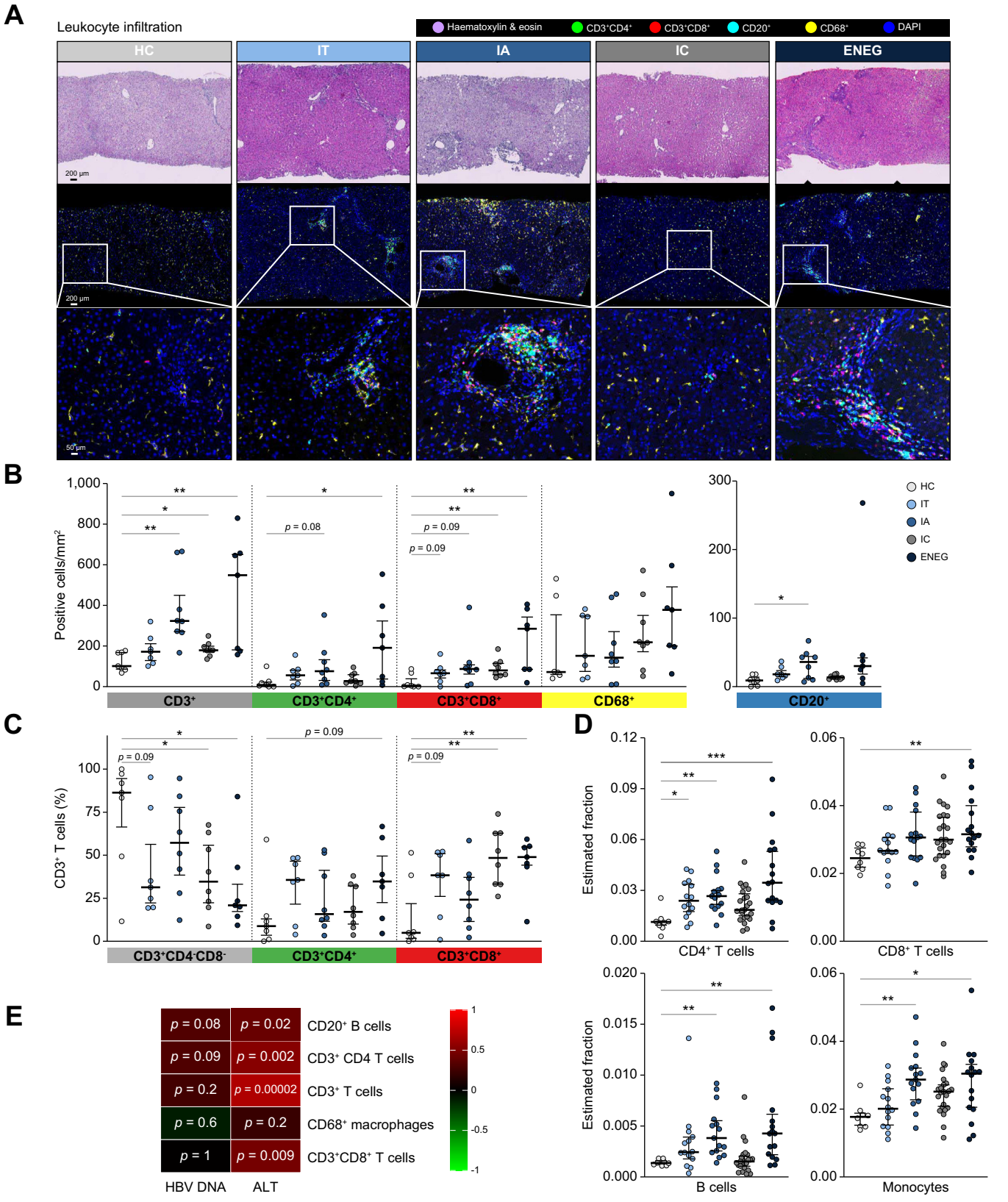

Fig. 3. Leukocyte infiltration is increased across chronic HBV natural history and correlates with serum ALT. (A) Leukocyte infiltration by multiplex immunofluorescence staining from HC and chronic HBV phases displaying T cells ($CD3^+CD4^+$ and $CD3^+CD8^+$, green and red, respectively), macrophages ($CD68^+$; yellow) and B cells ($CD20^+$; teal). (B) Density of cells per mm^2 positive for CD3, CD4, CD8 T cells, CD20 B cells and CD68 macrophages. (C) Percentage of $CD4^-CD8^-$ T cells, CD4 and CD8 T-cell subsets and in chronic HBV and healthy livers. (D) *In silico* EPIC estimated fractions of bulk leukocyte populations: CD4 and CD8 T cells, B cells and macrophages/monocytes. (E) Spearman correlations between peripheral biomarkers (HBV DNA and ALT) and leukocyte infiltrate (number of $CD3^+$ cells,

biopsies per phase, Fig. 3A, Table S1). In liver biopsies from healthy controls, T-cell (mean 122 cells/mm^2) and B-cell (mean 9 cells/mm^2) immune subsets were primarily found around portal areas, while CD68 Kupffer cells and macrophages were present across the liver parenchyma (Fig. 3A). However, liver biopsies across all chronic HBV phases showed increased evidence of immune cell activity. The IT and IC groups showed a modest increase in immune cell densities: T cells (mean 182 and 185 T cells/mm^2), B cells (mean 20 and 14 cells/mm^2) and macrophages (mean 202 and 264 cells/ mm^2). Consistent with previous observations, liver biopsies from patients belonging to the IA and ENEG groups showed pronounced infiltration predominantly around portal and periportal areas (T cells [mean 383 and 458 T cells/mm^2], B cells [mean 33 and 61 cells/mm^2]), while macrophages (mean 193 and 396 cells/mm^2) were found both around portal structures and dispersed across the parenchyma (Fig. 3A). Analysis of the staining profiles in chronic HBV livers demonstrated that compared to healthy livers, the number of total CD3$^+$ T cells showed an increase in all chronic HBV phases, albeit that the increase was not statistically significant in IT patients (Fig. 3B). In contrast, the number of CD8$^+$ T cells was significantly increased in HBeAg-negative patients (IC and ENEG) whereas CD4$^+$ T cells showed an increased trend in phases with active inflammation (IA and ENEG, p = 0.08 and p <0.05, respectively). These increased trends observed in the CD4$^+$ and CD8$^+$ T-cell subsets were further accentuated when expressed as a percentage of the total CD3 T cells. Interestingly, the frequency of CD4 and CD8 T cells in the vast majority of healthy livers was less than 25% resulting in a larger proportion of double-negative CD4 and CD8 T cells, possible NKT and/or mucosal-associated invariant T (MAIT) cells, than in chronic HBV livers (Fig. 3C). CD20$^+$ B-cells showed a comparable trend as CD4$^+$ T cells, albeit in lower numbers, as the ENEG phase showed the greatest increase. Moreover, the number of macrophages and those positive for PD-L1, linked to induce immune-exhaustion/impairment in chronic viral infections,[28] remained comparable in livers of healthy individuals and across chronic HBV phases (Fig. 3B and S4). Similarly, the number of CD3 T cells positive for PD-1 remained constant across chronic HBV phases and to a comparable level observed in healthy control livers (Fig. S4). Moreover, the *in silico* estimated fractions, by EPIC, of the different T-cell subsets (CD4 and CD8), B cells and monocytes highlighted a similar pattern of increased leukocyte infiltrate in chronic HBV, further elevated in IA and ENEG, as observed by mIF (Fig. 3D). Not surprisingly we observed significant positive associations (rho ≥0.5) between the number of detected leukocytes per mm^2 and the transcriptome-based estimated fractions (EPIC) (Fig. S5).

Interestingly, the higher degree of heterogeneity in leukocyte infiltrate (number of CD4$^+$ and CD8$^+$ T cells), which was seen in chronic inflammation phases (IA and ENEG) partially coincided with higher serum ALT levels. Indeed, correlation analysis highlighted the significant positive association between leukocyte infiltration (B cells, T cells and CD4 and CD8 T-cell subsets) and serum ALT levels (Fig. 3E). In contrast, none of the infiltrating leukocyte populations correlated with serum HBV DNA (Fig. 3E).

Intrahepatic viral antigens are heterogeneously expressed across and within CHB natural history phases and do not correlate with leukocyte infiltrate

Previous results have highlighted liver inflammation as the main driver in the highly differential transcriptomic and leukocyte infiltrate profiles seen in chronic HBV livers. However, whether these inflammatory processes are correlated with the intrahepatic expression of the viral proteins HBsAg and HBcAg remains unclear. To that end, we first performed systematic analysis of the viral staining pattern in HBV biopsies in the context of the different chronic HBV phases. We analyzed viral antigen proteins in the liver as part of the mIF assay by detecting HBsAg and HBcAg and further evaluated the parameters that correlate with the observed liver inflammation.

Infected hepatocytes were detected by positivity for HBsAg and/or HBcAg using Na/K-ATPase, panCK and CD299 as segmentation markers to selectively guide hepatocyte classification at the single cell level (Fig. S6). Heterogeneous expression of surface and/or cytoplasmic HBsAg was detected in infected liver biopsies across all stages of HBV (Fig. 4A). Upon quantification using digital image analysis tools on the stained images, a gradual decline in the percentage of infected hepatocytes from IT, IA, IC to ENEG phases was seen (Fig. 4B). The percentage of hepatocytes stained positive for HBsAg tended to decline over the course of chronic HBV (mean IT: 57%, IA: 30%, IC: 32% and ENEG: 27%), but was highly heterogeneous within and across groups (Fig. 4B). As expected, HBcAg-positive hepatocytes were identified only in IT and IA patients (mean IT: 70%, IA: 51%; Fig. 4B). To note, HBcAg detection was predominantly localized in the cytoplasm of infected hepatocytes and rarely in the nucleus (nuclear HBcAg in infected cells <25% in 7/7 IT; 6/8 IA; 6/7 ENEG; 7/7 IC patients) (Fig. S6). In contrast, HBsAg was heterogeneously detected in the membrane and cytoplasm of infected cells (Fig. S6). Moreover, as presented in Fig. 4C, the transcriptome-based detected integration of HBV DNA in the host genome (chimeric reads) is relatively constant over the course of chronic infection, while the total non-integrated HBV reads are highest in IT and IA, suggesting that this distinct pattern in HBcAg protein expression is predominantly driven by non-integrated forms of HBV.

When we performed correlation analysis to determine whether the degree of liver inflammation correlated with the intrahepatic expression of HBcAg and HBsAg, no correlation was found between any of the leukocyte populations and the HBV viral proteins HBcAg and HBsAg (Fig. 4D). However, we found a strong correlation between HBcAg and HBV DNA (p <0.001; r^2=0.864) but interestingly, no correlation with HBsAg levels (Fig. 4D). Together, these results demonstrate that the degree of liver damage but not HBV virological markers is associated with the degree of leukocyte infiltration in chronic HBV livers.

Discussion

The present study examines in detail the intrahepatic interplay between HBV and the host-immune response in all 4 phases of chronic HBV. Through mIF and liver transcriptome analysis (RNA-

T-cell subsets (CD4$^+$ and CD8$^+$), CD20$^+$ B-cells and CD68$^+$ macrophages per mm^2) in chronic HBV livers. Correlation Rho coefficients are color-coded as a transitional gradient from red (Rho >1) to green (Rho <0). p values for each correlation pair are displayed within each quadrant. Panel B-D display median and IQR bars. *p <0.05, **p <0.01, ***p <0.001; Unpaired t test compared to healthy samples for panels B, C and D. IQR is shown. ALT, alanine aminotransferase; ENEG; HBeAg-negative hepatitis; HC, healthy control; IA, immune-active; IC, inactive carrier IT, immunotolerant.

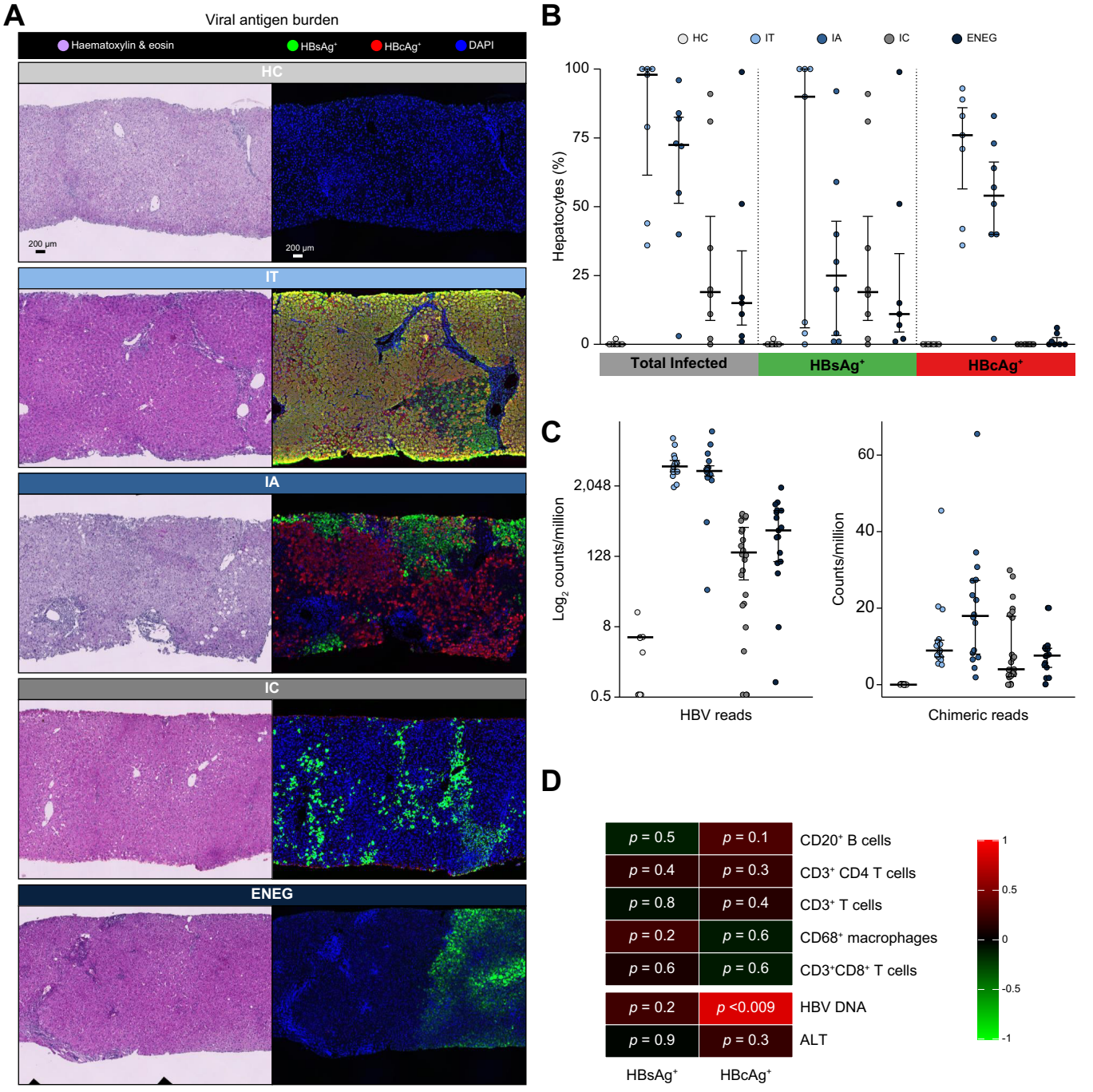

Fig. 4. Intrahepatic viral antigens are heterogeneously expressed in chronic HBV livers and do not correlate with leukocyte infiltrate. (A) HBcAg (red) and HBsAg (green) immunofluorescence staining overlays representative of liver biopsies from healthy individuals and chronic HBV phases. (B) Percentage of hepatocytes positive for HBcAg and/or HBsAg in chronic HBV livers. (C) Number of HBV and host-integrated (chimeric) reads (expressed as counts per million) in chronic HBV phases. (D) Spearman correlation between HBV viral burden (percentage of hepatocytes positive for HBcAg or HBsAg) and the leukocyte infiltrate (number of $CD3^+$ cells, T-cell subsets [$CD4^+$ and $CD8^+$], $CD20^+$ B cells and $CD68^+$ macrophages per mm^2) in chronic HBV livers. Correlation Rho coefficients are color-coded as a transitional gradient from red (Rho >1) to green (Rho <0). Panel B-C display median and IQR bars. *p* values for each correlation pair are displayed within each quadrant. IQR is shown. ALT, alanine aminotransferase; ENEG; HBeAg-negative hepatitis; HC, healthy control; IA, immune-active; IC, inactive carrier IT, immunotolerant.

seq) we show that livers of patients in the IT and IC phase show modest levels of CD3 T-cell infiltration and an altered immune gene expression profile when compared to healthy livers. These changes found in IT and IC livers with respect to their healthy counterparts were more pronounced in IA and ENEG livers, where serum ALT, but not serum HBV DNA or intrahepatic HBV proteins (HBsAg and HBcAg) correlated with leukocyte inflammation. Besides innate and adaptive immune genes, an upregulation of genes encoding for immune-exhaustion markers was also observed in IA and ENEG livers, with the highest increase in ENEG. All chronic

HBV phases showed a common suppression of metabolic gene sets compared to healthy livers. Moreover, all chronic HBV phases, in particular IA and ENEG phases, showed reduced expression of complement genes.

In contrast to the current view in which HBV can increase metabolic signaling pathways such as lipogenesis via viral proteins such as HBx[29] we demonstrate suppression of liver metabolic gene sets such as fatty/lipid and bile acid metabolism or response to toxic substrates in all chronic HBV phases. A possible explanation for this observation is that the current understanding is largely supported by *in vitro* studies with HBV-infected hepatoma cell lines, which may not reflect the intrinsic complexity of chronic HBV disease in human livers. Furthermore, a recent study evaluating the transcriptomic changes over time in distinct liver-injury mouse models showed metabolic gene and pathway downregulation coinciding with the induction of inflammatory pathways. This was later confirmed in various etiologies in human livers, including HBV infection.[30] Consistent with this study, we observed the strongest metabolic downregulation in those phases accompanied by increased inflammation. Moreover, metabolomics studies have shown a deregulated serum lipid profile with strong downregulation of specific lipid metabolites in patients with chronic HBV compared to controls.[31,32] However, it cannot be excluded that a more extensive infiltrate in the liver may alter the transcriptomic input from parenchymal cells leading to the observed reduced expression of metabolic genes compared to healthy livers in our analysis. Single-cell RNA-seq of liver parenchymal cells and/or spatial transcriptomics may provide more detailed information needed to resolve this issue.

Besides the downregulation of metabolic gene sets in chronic HBV, we observed a general upregulation of diverse innate and adaptive immune genes in chronic HBV, albeit only statistically significant in livers from IA and ENEG phases when compared to healthy livers. These results are in stark contrast with the transcriptomic characterization of chronic HBV livers conducted by Lebossé *et al.*, where a large number of innate immune genes (*i.e.*, ISGs, TLR-related) were downregulated in livers of patients with chronic HBV compared to non-viral infected controls.[14] Of note, whereas we included core needle liver biopsies from altruistic liver donors as healthy uninfected controls, Lebossé's study included, as controls, liver material from a mix of 6 patients with gallbladder stones, 1 with ovarian cystadenoma and 2 with non-metastatic colon cancer who underwent liver surgery, in whom inflammatory processes were likely to be ongoing.[14]

Interestingly, the transcriptomic profile we observed in HBV phases was highly homogeneous across patients despite fluctuating levels of serum biomarkers such as HBV DNA and ALT. Hence the fluctuating serological profile characteristic of these phases is not mirrored by changes in the intrahepatic transcriptome. However, this observation might be at least partially explained by the moment in which the liver biopsy was taken in relation to when the ongoing inflammation in the liver started. Moreover, inflammatory chemokines encoding genes such as *CXCL10* and *CXCL9,* as well as several innate and adaptive immune genes, were found to be upregulated in IA and ENEG phases suggesting that these phases are immunologically more active. Further strengthening this view, we found T-cell activation genes such as *ICOS*, *ITK* and PDK1 to be upregulated. However, a number immune exhaustion-encoding genes were also found to be upregulated in livers in the IA and ENEG phases. Besides genes encoding markers previously observed to be expressed in HBV-specific T cells (*PDCD1*, *CTLA4*, *LGALS9*) *TOX* was also observed, paralleling a recently identified transcription factor preferentially found in phenotypically and functionally exhausted HBV-specific CD8+ T cells.[33] Furthermore, newly identified genes were observed that encoded for other T cell-related immune exhaustion or inhibitory markers, such as *SLAMF7*, *SLAMF6*, *TNFRSF9, TNFAIP2* and *TNFAIP3*.[34–38] A larger proportion of these genes were found to be upregulated in ENEG livers which indicates that minor but significant differences may be present in the T-cell responses between IA and ENEG phases.

For the first time, we now demonstrate an increased number of T cells in livers at chronic HBV phases which were further increased in phases with elevated ALT (IA and ENEG) when compared to healthy livers, contrary to the comparable frequencies of leukocyte subsets in blood across chronic HBV phases.[5–7] In contrast, we detected lower frequencies of CD4CD8 double-negative T cells in all livers from chronic HBV phases compared to healthy livers. Whether this population represents NKT and/or MAIT cells, which can comprise up to 15% of the intrahepatic leukocytes,[39,40] and their functional status warrants further investigation. However, other chronic viral infections such as HIV and HCV are associated with lower peripheral and intrahepatic MAIT frequencies, with a more exhausted phenotype compared to healthy controls.[41,42] Moreover, some livers from patients classified in the IA and ENEG phase displayed immune infiltrate levels comparable to uninfected controls despite the homogeneity in their transcriptome. Interestingly, leukocyte infiltration positively associated with serum ALT levels, but not with serum HBV DNA and intrahepatic HBcAg and HBsAg protein expression. This disconnect between intrahepatic immune profiles and viral markers strengthens our previous observation in which intrahepatic HBsAg expression minimally altered the transcriptome in the IC livers.[43] Furthermore, the positive association seen for the leukocyte infiltrate and serum ALT levels coincides with the paradigm in which immune-mediated liver damage induces ALT release by dying hepatocytes.[1] However, further studies are warranted to better understand whether the limited but detectable T-cell infiltrate present in IT and IC phases affects intrahepatic responses and initiates cytopathic damage. In addition, the underlying mechanisms that trigger the inflammatory response during an ongoing HBV infection in the absence of antiviral treatment warrant further investigation. Further studies are needed to confirm these findings, for instance by sampling the liver via fine needle aspirates, and analysis by multi-color flowcytometry and scRNA-Seq .[11]

In summary, the comprehensive characterization of a unique cohort of livers of healthy individuals and patients with chronic HBV revealed a previously unreported increase in leukocyte infiltrate and immune gene expression in chronic HBV phases, and downregulation of metabolic gene sets when compared to healthy controls. These increased immune-gene profiles were significantly accentuated in IA and ENEG livers which showed a common upregulated profile of innate (ISGs, antiviral) and adaptive immune (T-/B-cell) genes, while immune-exhaustion and inhibitory genes were most pronounced in ENEG livers. Given the increased interest in HBV studies using liver tissue instead of blood, our comprehensive analysis from a large group of well-defined liver biopsies serves as a starting point for future

more detailed studies at the single cell level. Our results show the heterogeneity of intrahepatic processes in the different phases, which needs to be considered in ongoing efforts to improve treatment strategies for chronic HBV.

Abbreviations

ALT, alanine aminotransferase; BP, biological process; DEG, differentially expressed gene; EASL, European Association for the Study of the Liver; ENEG; HBeAg-negative hepatitis; FFPE, formalin-fixed paraffin-embedded; GSEA, gene set-enrichment analysis; IA, immune-active; IC, inactive carrier; IRF, interferon-regulatory factor; ISG, interferon-stimulate gene; IT, immunotolerant; MAIT, mucosal-associated T cell; NK, natural killer; RNA-sequencing; RNA-seq.

Financial support

This work was funded by Foundation for Liver and Gastrointestinal Research (AB) and Robert Wood Johnson Foundation, Harold Amos Medical Faculty Development Program and University of Minnesota AIRP grant (JDD).

Conflict of interest

NRM, MD and JDD declare no conflict of interest. AB received grant support from Janssen, GSK, Fujirebio and Gilead Sciences, Inc. At the time this study was conducted, RR, NVB, AA, CM, ST, LD, LL and BF were employees and stockholders of Gilead Sciences, Inc.

Please refer to the accompanying ICMJE disclosure forms for further details.

Authors' contributions

NRM and AB designed the study. MD provided liver FFPE tissues and conducted histological examination. AA and CM developed and optimized 12-plex immunofluorescence staining on FFPE liver-biopsies; AA, ST and LD analyzed the data. RR and NVB overlooked and organized RNA-sequencing. NRM and RR conducted RNA-seq analysis. NRM and AB wrote the manuscript. NRM, RR, NVB, MD, AA, JD, BF and AB critically revised the manuscript. AB and BF secured funding. All authors approved the final version of the manuscript.

Data availability statement

The raw data that support the findings of this study will be uploaded in a public repository, like GEO, upon acceptance of the manuscript.

Acknowledgments

We would like to thank Dr. Arlin Keo for her assistance during transcriptome analysis, and the teams at Ultivue (CA, USA) and OracleBio (Scotland, UK) for the multiplex immunofluorescence studies and analysis, and Sarah Tse from Bioscience Communications for the high-quality figures.

Supplementary data

Supplementary data to this article can be found online at https://doi.org/10.1016/j.jhep.2022.02.016.

References

Author names in bold designate shared co-first authorship

[1] Guidotti LG, Chisari FV. Immunology and pathogenesis of viral hepatitis. Annu Rev Pathol Mech Dis 2006;1:23–61.
[2] Hoofnagle JH, Doo E, Liang TJ, Fleischer R, Lok ASF. Management of hepatitis B: summary of a clinical research workshop. Hepatology 2007;45:1056–1075.
[3] Lampertico P, Agarwal K, Berg T, Buti M, Janssen HLA, Papatheodoridis G, et al. EASL 2017 Clinical Practice Guidelines on the management of hepatitis B virus infection. J Hepatol 2017;67:370–398.
[4] Giadans CG, Ríos DA, Ameigeiras B, Pietrantonio AM, Lucatelli NL, Haddad L, et al. Chronic hepatitis B: the interplay between intrahepatic lymphocyte population and viral antigens in relation to liver damage. J Viral Hepat 2019;26:727–737.
[5] Vanwolleghem T, Groothuismink ZMA, Kreefft K, Hung M, Novikov N, Boonstra A. Hepatitis B core-specific memory B cell responses associate with clinical parameters in patients with chronic HBV. J Hepatol 2020;73:52–61.
[6] de Groen RA, Hou J, van Oord GW, Groothuismink ZMA, van der Heide M, de Knegt RJ, et al. NK cell phenotypic and functional shifts coincide with specific clinical phases in the natural history of chronic HBV infection. Antivir Res 2017;140:18–24.
[7] Wang W-T, Zhao X-Q, Li G-P, Chen Y-Z, Wang L, Han M-F, et al. Immune response pattern varies with the natural history of chronic hepatitis B. World J Gastroenterol 2019;25:1950–1963.
[8] Boeijen LL, Hoogeveen RC, Boonstra A, Lauer GM. Hepatitis B virus infection and the immune response: the big questions. Best Pract Res Clin Gastroenterol 2017;31:265–272.
[9] Gill US, Pallett LJ, Thomas N, Burton AR, Patel AA, Yona S, et al. Fine needle aspirates comprehensively sample intrahepatic immunity. Gut 2019;68:1493–1503.
[10] Pallett LJ, Davies J, Colbeck EJ, Robertson F, Hansi N, Easom NJW, et al. IL-2(high) tissue-resident T cells in the human liver: sentinels for hepatotropic infection. J Exp Med 2017;214:1567–1580.
[11] Boeijen LL, van Oord GW, Hou J, van der Heide-Mulder M, Gaggar A, Li L, et al. Gene expression profiling of human tissue-resident immune cells: comparing blood and liver. J Leukoc Biol 2019;105:603–608.
[12] Hou J, Brouwer WP, Kreefft K, Gama L, Price SL, Janssen HLA, et al. Unique intrahepatic transcriptomics profiles discriminate the clinical phases of a chronic HBV infection. PLoS One 2017;12:e0179920. e0179920.
[13] Liu H, Li F, Zhang X, Yu J, Wang J, Jia J, et al. Differentially expressed intrahepatic genes contribute to control of hepatitis B virus replication in the inactive carrier phase. J Infect Dis 2018;217:1044–1054.
[14] Lebossé F, Testoni B, Fresquet J, Facchetti F, Galmozzi E, Fournier M, et al. Intrahepatic innate immune response pathways are downregulated in untreated chronic hepatitis B. J Hepatol 2017;66:897–909.
[15] Brouwer WP, van der Meer AJ, Boonstra A, Pas SD, de Knegt RJ, de Man RA, et al. The impact of PNPLA3 (rs738409 C>G) polymorphisms on liver histology and long-term clinical outcome in chronic hepatitis B patients. Liver Int Off J Int Assoc Study Liver 2015;35:438–447.
[16] Haeussler M, Zweig AS, Tyner C, Speir ML, Rosenbloom KR, Raney BJ, et al. The UCSC Genome Browser database: 2019 update. Nucleic Acids Res 2019;47:D853–D858.
[17] Broad Institute. Picard toolkit. GitHub Repos: Broad Institute; 2019.
[18] Liao Y, Smyth GK, Shi W. featureCounts: an efficient general purpose program for assigning sequence reads to genomic features. Bioinformatics 2014;30:923–930.
[19] **Robinson MD**, **McCarthy DJ**, Smyth GK. edgeR: a Bioconductor package for differential expression analysis of digital gene expression data. Bioinformatics 2010;26:139–140.
[20] Hänzelmann S, Castelo R, Guinney J. GSVA: gene set variation analysis for microarray and RNA-Seq data. BMC Bioinformatics 2013;14:7.
[21] Love MI, Huber W, Anders S. Moderated estimation of fold change and dispersion for RNA-seq data with DESeq2. Genome Biol 2014;15:550.
[22] Subramanian A, Tamayo P, Mootha VK, Mukherjee S, Ebert BL, Gillette MA, et al. Gene set enrichment analysis: a knowledge-based approach for interpreting genome-wide expression profiles. Proc Natl Acad Sci 2005;102:15545–15550.

[23] Racle J, Gfeller D. EPIC: a tool to estimate the proportions of different cell types from bulk gene expression data. Methods Mol Biol 2020;2120:233–248.
[24] Sturm G, Finotello F, List M. Immunedeconv: an R package for unified access to computational methods for estimating immune cell fractions from bulk RNA-sequencing data. Methods Mol Biol 2020;2120:223–232.
[25] Manesse M, Patel KK, Bobrow M, Downing SR. The InSituPlex(®) staining method for multiplexed immunofluorescence cell phenotyping and spatial profiling of tumor FFPE samples. Methods Mol Biol 2020;2055:585–592.
[26] Wharton KAJ, Wood D, Manesse M, Maclean KH, Leiss F, Zuraw A. Tissue multiplex analyte detection in anatomic pathology - pathways to clinical implementation. Front Mol Biosci 2021;8:672531.
[27] Vasaturo A, Galon J. Multiplexed immunohistochemistry for immune cell phenotyping, quantification and spatial distribution in situ. Methods Enzymol 2020;635:51–66.
[28] Said EA, Al-Reesi I, Al-Riyami M, Al-Naamani K, Al-Sinawi S, Al-Balushi MS, et al. A potential inhibitory profile of liver CD68+ cells during HCV infection as observed by an increased CD80 and PD-L1 but not CD86 expression. PLoS One 2016;11:e0153191.
[29] Shi Y-X, Huang C-J, Yang Z-G. Impact of hepatitis B virus infection on hepatic metabolic signaling pathway. World J Gastroenterol 2016;22:8161–8167.
[30] Campos G, Schmidt-Heck W, De Smedt J, Widera A, Ghallab A, Pütter L, et al. Inflammation-associated suppression of metabolic gene networks in acute and chronic liver disease. Arch Toxicol 2020;94:205–217.
[31] Arain SQ, Talpur FN, Channa NA, Ali MS, Afridi HI. Serum lipids as an indicator for the alteration of liver function in patients with hepatitis B. Lipids Health Dis 2018;17:36.
[32] Schoeman JC, Hou J, Harms AC, Vreeken RJ, Berger R, Hankemeier T, et al. Metabolic characterization of the natural progression of chronic hepatitis B. Genome Med 2016;8:64.
[33] Heim K, Binder B, Sagar, Wieland D, Hensel N, Llewellyn-Lacey S, et al. TOX defines the degree of CD8+ T cell dysfunction in distinct phases of chronic HBV infection. Gut 2020:gutjnl-2020-322404.
[34] Kim H-D, Park S, Jeong S, Lee YJ, Lee H, Kim CG, et al. 4-1BB delineates distinct activation status of exhausted tumor-infiltrating CD8(+) T cells in hepatocellular carcinoma. Hepatology 2020;71:955–971.
[35] Awwad MHS, Mahmoud A, Bruns H, Echchannaoui H, Kriegsmann K, Lutz R, et al. Selective elimination of immunosuppressive T cells in patients with multiple myeloma. Leukemia 2021.
[36] Miller BC, Sen DR, Al Abosy R, Bi K, Virkud YV, LaFleur MW, et al. Subsets of exhausted CD8(+) T cells differentially mediate tumor control and respond to checkpoint blockade. Nat Immunol 2019;20:326–336.
[37] Just S, Nishanth G, Buchbinder JH, Wang X, Naumann M, Lavrik I, et al. A20 curtails primary but augments secondary CD8+ T cell responses in intracellular bacterial infection. Sci Rep 2016;6:39796.
[38] Martinez GJ, Pereira RM, Äijö T, Kim EY, Marangoni F, Pipkin ME, et al. The transcription factor NFAT promotes exhaustion of activated CD8^{+} T cells. Immunity 2015;42:265–278.
[39] Jo J, Tan AT, Ussher JE, Sandalova E, Tang X-Z, Tan-Garcia A, et al. Toll-like receptor 8 agonist and bacteria trigger potent activation of innate immune cells in human liver. Plos Pathog 2014;10:e1004210.
[40] Jeffery HC, van Wilgenburg B, Kurioka A, Parekh K, Stirling K, Roberts S, et al. Biliary epithelium and liver B cells exposed to bacteria activate intrahepatic MAIT cells through MR1. J Hepatol 2016;64:1118–1127.
[41] Bolte FJ, O'Keefe AC, Webb LM, Serti E, Rivera E, Liang TJ, et al. Intra-Hepatic depletion of mucosal-associated invariant T cells in hepatitis C virus-induced liver inflammation. Gastroenterology 2017;153:1392–1403.e2.
[42] Eberhard JM, Kummer S, Hartjen P, Hüfner A, Diedrich T, Degen O, et al. Reduced CD161(+) MAIT cell frequencies in HCV and HIV/HCV co-infection: is the liver the heart of the matter? J Hepatol 2016;65:1261–1263.
[43] Rico Montanari N, Ramirez R, Van Buuren N, van den Bosch TPP, Doukas M, Debes JD, et al. Transcriptomic analysis of livers of Inactive Carrier HBV patients with differential HBsAg. J Infect Dis 2021.